Title

Regulation of human cerebral cortical development by EXOC7 and EXOC8, components of the exocyst complex, and roles in neural progenitor cell proliferation and survival

Journal

Genetics in Medicine, 22(6)

ISSN

1098-3600

Authors

Coulter, Michael E
Musaev, Damir
DeGennaro, Ellen M
et al.

Publication Date

2020-06-01

DOI

10.1038/s41436-020-0758-9

Peer reviewed

Regulation of human neural progenitor cell proliferation and survival by *EXOC7* and *EXOC8*, components of the exocyst complex

Michael E. Coulter[1,2], Damir Musaev[3], Ellen M. DeGennaro[1,12], Xiaochang Zhang[1,4], Katrin Henke[5], Kiely James[3], Richard S. Smith[1], R. Sean Hill[1], Jennifer N. Partlow[1], Muna Al-Saffar[1, 10], Stacy Kamumbu[1], Nicole Hatem[1], A. James Barkovich[6], Maha S. Zaki[7], Tipu Sultan[8], Anna Rajab[9], Lihadh Al-Gazali[10], Ganeshwaran H. Mochida[1,11], Matthew P. Harris[5], Joseph G. Gleeson[3]*, Christopher A. Walsh[1]*

1. Division of Genetics and Genomics and Howard Hughes Medical Institute, Boston Children's Hospital, Departments of Pediatrics and Neurology, Harvard Medical School, Boston, MA 02115, USA
2. Program in Neuroscience and Harvard/MIT MD-PHD Program, Harvard Medical School, Boston, MA 02115, USA
3. Department of Neurosciences and Howard Hughes Medical Institute, University of San Diego, La Jolla, CA 92093, USA
4. Department of Human Genetics, University of Chicago, Chicago, IL 60637, USA
5. Division of Orthopedic Research, Boston Children's Hospital, Department of Genetics, Harvard Medical School, Boston, MA 02115, USA
6. Benioff Children's Hospital, Departments of Radiology, Pediatrics, Neurology, and Neurological Surgery, University of California San Francisco, San Francisco, CA 94158, USA
7. Clinical Genetics Department, Human Genetics and Genome Research Division, National Research Centre, Cairo 12311, Egypt
8. Department of Pediatric Neurology, Institute of Child Health & The Children's Hospital, Lahore, 54000, Pakistan
9. National Genetics Center, Directorate General of Health Affairs, Ministry of Health, Muscat, Oman
10. Department of Paediatrics, College of Medicine and Health Sciences, United Arab Emirates University, Al Ain, United Arab Emirates
11. Department of Neurology, Massachusetts General Hospital, Boston, MA 02114, USA
12. Harvard-MIT Division of Health Sciences and Technology, Massachusetts Institute of Technology, Cambridge, Massachusetts, USA

***Corresponding Authors:**

Christopher A. Walsh

Division of Genetics and Genomics

Boston Children's Hospital

300 Longwood Avenue, BCH3150

Boston, MA 02115 USA

Email: christopher.walsh@childrens.harvard.edu

Joseph G. Gleeson

Department of Neurosciences

University of California, San Diego

9500 Gilman Drive #0665

La Jolla, CA 92093-0665

Email: jogleeson@ucsd.edu

ABSTRACT

The exocyst complex is a conserved protein complex that mediates fusion of intracellular vesicles to the plasma membrane and is implicated in processes including cell polarity, cell migration, ciliogenesis, cytokinesis, autophagy, and fusion of secretory vesicles. Here, we report mutations in two members of the exocyst complex, *EXOC7* (*EXO70*) and *EXOC8 (EXO84)*, in a novel brain development disorder that affects the maturation and differentiation of cells in the cerebral cortex. In *EXOC7*, we identified three independent partial loss of function (LOF) mutations in three families with a recessively inherited brain developmental disorder characterized by brain atrophy, seizures, and developmental delay, and in more severe cases microcephaly and infantile death. In *EXOC8*, we found a homozygous truncating mutation in a family with a very similar clinical disorder. We modeled *exoc7* deficiency in zebrafish and found that the absence of *exoc7* causes microcephaly with increased apoptosis and loss of progenitor cells in the developing telencephalon. Together, these findings highlight the essential role of the exocyst pathway in normal cortical development and how its perturbation causes complex brain disorders.

INTRODUCTION

Eight genes in the human genome, *EXOC1* – *EXOC8*, encode the exocyst complex, a multimeric, evolutionarily-conserved complex that traffics vesicles within the cell to the plasma membrane for fusion. The exocyst complex has been shown to play a role in several cellular processes, including cell polarity, cell migration, ciliogenesis, cytokinesis, autophagy, and fusion of secretory vesicles (reviewed in Polgar and Fogelgren, 2018), but disorders associated with definitive loss-of-function mutations in any of these components have not yet been reported. Although a missense mutation in *EXOC8* [MIM: 615283] was reported in a single case of Joubert syndrome (Dixon-Salazar et al., 2012), and a missense mutation in *EXOC4* [MIM: 608185] was reported in a case of Meckel-Gruber syndrome (Shaheen et al., 2013), the pathogenicity of these two mutations has not yet been confirmed. As such, the role of individual proteins of the exocyst complex remains unclear.

Several of the reported functions of the exocyst complex, cell polarity and migration (Dupraz et al., 2009; Fujita et al., 2013; Liu et al., 2012), cytokinesis (Polgar and Fogelgren, 2018), and ciliogenesis (Polgar and Fogelgren, 2018) are integral processes during cerebral cortical development and so motivated us to test the hypothesis that mutations in exocyst encoding genes cause brain development disorders. First, establishing cell polarity and cell migration are essential for cortical development. The classic bipolar shape of radial glial cell progenitors (RGC) specifies asymmetric and

symmetric progenitor cell divisions, and supports the radial migration of newborn neurons. Mutations in RGC polarity genes, such as *Pals1* and *Par3*, disrupt cortical development through massive cell death or premature cell cycle exit, respectively (Kim et al., 2010; Costa et al., 2008). In addition, many genes that are required for neuronal migration also regulate RGC polarity, and when mutated can cause one of several cortical malformations, including lissencephaly (*PAFAH1B1/LIS1* [MIM: 607432], Reiner et al., 1993), double cortex syndrome (*DCX* [MIM: 300121], Gleeson et al., 1998; des Portes et al., 1998), and cortical dysplasia (*TUBB3* [MIM: 602661], *TUBB5* [MIM: 191130], *KIF5C* [MIM: 604593], *KIF2A* [MIM: 602591], Breuss et al., 2012; Poirier et al., 2010; Poirier et al., 2013). Second, robust and rapid cell division of cortical progenitors is essential for cortical development and several genetic causes of microcephaly exhibit disrupted cytokinesis as a result of supernumerary (*CDK5RAP2* [MIM: 608201], *KATNB1* [MIM: 602703], Lizarraga et al. 2010; Pagnamenta et al. 2012, Hu et al. 2014; Mishra-Gorur et al. 2014), or missing spindle poles (*ASPM* [MIM: 605481], *WDR62* [MIM: 613583], Bond et al. 2002, Bhat et al. 2011; Jayaraman et al. 2016). Finally, defects in cilia formation lead to a group of syndromes called ciliopathies, complex syndromes that include disrupted brain development (*INPP5E* [MIM: 613037], *C2CD3* [MIM: 615944], *BBS1* [MIM: 209901], Bielas et al., 2009, Thauvin-Robinet et al., 2014, Muller et al., 2010).

Here we provide a systematic analysis of mutations in multiple exocyst components, by defining several mutations in *EXOC7* [MIM: 608163] and

EXOC8 [MIM: 615283]. We identify three independent mutations in *EXOC7*, all likely separately to confer partial loss-of-function, associated with developmental brain disorders of variable severity characterized by developmental delay, seizures, brain atrophy, microcephaly, and infantile death. We also describe one loss-of-function mutation in *EXOC8* similarly associated with severe developmental delay, seizures, brain atrophy, microcephaly, and premature death. We further provide a zebrafish genetic model of *EXOC7* loss-of-function and offer the first genetic evidence that *EXOC7* is required for neuron survival.

MATERIALS AND METHODS

IRB approval of human genetics

Operating under approved institutional review board (IRB) protocols at Boston Children's Hospital, University of California San Diego and the Faculty of Medicine, United Arab Emirates University, blood samples were collected from all individuals included in the study.

IACUC approval of zebrafish housing and experiments

A complete description of the husbandry and environmental conditions in housing for the fish used in these experiments is available as a collection in protocols.io dx.doi.org/10.17504/protocols.io.mrjc54n. All animals were cared for humanly and all experiments were approved by Boston Children’s Hospital IACUC.

Whole exome sequencing

DNA was extracted from whole blood. Whole exome sequencing was performed at the Broad Institute with the following details. Families I, II, III: Agilent Sure-Select Human All Exon v2.0 capture kit and sequenced on Illumina HiSeqX with 76bp paired-end reads. Individual I-01: 76.5% of the target region was covered by at 20 or more reads, Individual I-05: 86.6% of the target region was covered by at 20 or more reads. Family IV: ICE capture with Nextera-based LC and sequenced on Illumina HiSeq4000 with 151bp paired-end reads. Individual IV-01: 91.6% of the target region was covered by at 20 or more reads, Individual IV-02: 93.1% of the target region was covered by at 20 or more reads. We filtered out variants with allele frequency >10% in Middle Eastern population (Scott et al., 2016).

Sanger sequencing

Primers surrounding the reported variant in each family were used for PCR and subsequent Sanger sequencing to confirm genotype from whole exome sequencing and determine segregation within the family.

Minigene cloning and expression

A ~5kb section of human *EXOC7* locus was amplified with primers (F: AAGGACTGAAGGAGCATTTC, R: CAGGGAGTCGAAGGTCTTCT) from a BAC containing the *EXOC7* locus and cloned into a mammalian expression vector. This vector was transfected into mouse N2A cells and after 48 hours RNA was isolated and then made into cDNA. N2A cells were cultured at 37 ˚C and 5% CO2 in high-glucose DMEM (GIBCO) supplemented with 10% fetal bovine serum and 1% penicillin-streptomycin.

HAP1 mutant cell line

HAP1 human cell line was cultured at 37 ℃ and 5% CO2 in high-glucose DMEM (GIBCO) supplemented with 10% fetal bovine serum and 1% penicillin-streptomycin. The splice acceptor mutation from Family I was introduced into a HAP1 cell line using CRISPR/Cas9 mutagenesis using techniques previous reported, and was present as a hemizygous mutation (Essletzbichler et al., 2014, Horizon Discovery).

***Exoc7* alternative splicing in developing cortex**

Alternative splicing analysis of *EXOC7* in developing human (GW13-16) and mouse (E14.5) cortex was performed as described previously (Zhang et al., 2016). Aligned BAM files from RNA sequencing datasets were analyzed with the MISO pipeline (version 0.4.6) to determine the inclusion frequency of alternatively spliced exons.

Generation of mutant zebrafish lines with CRISPR/Cas9 mutagenesis

Exoc7 mutant zebrafish were generated by CRISPR/Cas9 mutagenesis. Cas9 mRNA (250 ng/μl) and *exoc7* targeting guide RNA (target: CCGTCCTCATCCTGGACGCC, 80 ng/μl) were injected into 1-cell embryos. Embryos were allowed to develop to adulthood and then Sanger sequencing was used to identify potential heterozygous *exoc7* mutant carriers in F1 progeny. A 1-bp frameshift deletion in exon 5 was identified and this fish was backcrossed to WT to generate heterozygous carriers. The allele generated in this study is *mh111*.

Toluidine blue staining of developing zebrafish

5 dpf embryos were fixed in 4% PFA overnight at 4 ℃ and then embedded in JB-4 resin according to manufacturer's protocol (Polysciences Inc). Fish were sectioned at a thickness of 2 microns, and then matching sections were stained with toluidine blue and imaged with a bright-field microscope.

Immunostaining of progenitor cells in developing zebrafish

5 dpf embryos were fixed in 4% PFA overnight at 4 ℃, embedded in OCT, and cryo-sectioned coronally. Matched sections were stained with a primary antibody against Sox-2. Tissue was permeabilized and blocked in 3% BSA, 0.3% Triton X-100, 0.3% sodium azide in PBS. Primary antibodies were diluted in blocking buffer and incubated overnight at 4 ℃. Sections were then stained with Alexa secondary antibodies and Hoechst. Imaging was done on Zeiss 510 confocal microscope. Sox-2 positive nuclei within the telencephalon were counted.

TUNEL staining in developing zebrafish

5 dpf embryos were fixed in 4% PFA overnight at 4 ℃, embedded in OCT, and cryo-sectioned coronally. Apoptotic cells in matched sections were labeled with TUNEL staining using the Apoptag kit (Millipore) according to the manufactures instructions. Imaging was done on Zeiss 510 confocal microscope. TUNEL positive cells within the telencephalon were counted.

RNAscope

RNAscope on human fetal brain tissue was performed according to manufacturer's protocol (ACDBio). Tissue was fixed in 4% PFA, frozen, and sectioned at 20 um on a cryostat.

Quantification and Statistical Analysis

In all analyses, mean values are presented for pooled data and errors bars are SEM. For all quantifications, statistical significance was determined using a two-tailed, unpaired t-test. Except for 5F, which was calculated with two-way anova. Statistical analyses were performed using GraphPad Prism version 7.

RESULTS

EXOC7 and *EXOC8* mutations in recessive developmental disorders

In mapping developmental disorders affecting the cerebral cortex, we identified mutations in *EXOC7* and *EXOC8* associated with recessive brain development syndromes with a range of symptom severity including developmental delay, seizures, brain atrophy, microcephaly, and infantile death (**Table 1**).

Family I is a consanguineous family with the most severely affected children, having infantile lethality with neonatal micrencephaly, seizures, and arthrogryposis (**Figure 1A**). The family had two daughters who were born with myoclonic seizures and arthrogryposis multiplex. One had documented microcephaly (-2.7 SD), and both died within the first months of life (**Table 2**). Imaging of both siblings showed a cerebrum smaller than the skull cavity

with a thin cortex and extremely simplified gyri, enlarged ventricles, reduced white matter, and a very small cerebellum and brainstem. These findings are consistent with global cerebral cortical maldevelopment, as well as likely brain atrophy, reflecting neuronal loss (**Figure 1A**). Homozygosity mapping in this family identified a region on chromosome 17 linked to the disease with a statistically suggestive maximum LOD score of 1.93 (**Figure S1A**). Whole exome sequencing identified a homozygous splice mutation in *EXOC7* within this region (exon 7 splice acceptor, chr17:74087318 (hg19), C>T, c.809-2A>G, **Figure 1A**); this variant is heterozygous in 2/251,414 alleles from normal controls (frequency = 7.96×10^{-6}) and never homozygous (gnomAD database, Lek et al., 2016). This variant mutates a highly conserved base, disrupts the canonical splice acceptor for exon 7 (ag|G > gg|G), and segregates perfectly with disease in this family. One additional rare, homozygous variant was found in the same linkage region that caused a missense mutation in *CYB5D2* (chr17:4057982 (hg19), C>T, p.Arg136Trp), a gene that encodes a heme binding protein (Bruce and Rybak, 2014) with low expression in the developing cerebral cortex (**Figure 2S**). In the gnomAD database, this *CYB5D2* variant is heterozygous in 3/276,426 alleles from normal controls (frequency = 1.22×10^{-5}, 0 homozygous alleles), and there are 3 additional homozygous missense and 1 homozygous stop-gain variants in *CYB5D2* in gnomAD (Lek et al., 2016). Although little is known about *CYB5D2* function, its expression is much lower than *EXOC7* in

developing cortex and the greater relative severity of the *EXOC7* splice acceptor variant favor it as being causative in this family.

Family II has one affected male child, of consanguineous parents, with severe developmental delay, seizures, and mild microcephaly (-2.6 SD) (**Figure 1B**). His brain imaging showed central and cortical atrophy that is prominent in the temporal lobes (**Table 2**). Whole exome sequencing identified a homozygous 3-base pair deletion in exon 3 of *EXOC7* that removes a serine at position 48 (chr17:74097927-74097930 (hg19), GGAT>G, Ser48del, **Figure 1B**). This variant is heterozygous in 2/276,426 alleles from normal controls (frequency = 7.24×10^{-6}) and never homozygous (gnomAD database, Lek et al., 2016), and segregates perfectly with disease. In fact, the amino acid deleted by this mutation is within the CorEx motif of *EXOC7* (aa 5-67) (**Figure 1B**), which is thought to promote binding of EXOC7 to the protein encoded by *EXOC8* (EXO84), and is likely required for EXOC7-mediated assembly of the exocyst complex (Mei et al., 2018).

Family III is consanguineous with three siblings affected with recessively inherited seizures, intellectual disability, and developmental delay (**Figure 1C**). Brain imaging showed atrophy in two of the three affected siblings (**Table 2**). Homozygosity mapping identified a single linkage region on chromosome 17 with the maximum possible LOD score of 2.9. Whole exome sequencing identified a homozygous missense mutation in exon 15 of *EXOC7* within the linkage region (chr17:74081807 (hg19), C>T, Ala523Thr, **Figure 1C**). This variant is heterozygous in 2/277,066 alleles

from normal controls (frequency = 7.22×10^{-6}) and never homozygous (gnomAD database, Lek et al., 2016), and segregates perfectly with disease. Alanine 492 is a highly conserved amino acid that is conserved from humans to zebrafish.

Family IV exhibits recessively inherited global developmental delay with regression, seizures, and microcephaly in three daughters of consanguineous parents (**Figure 1D**). Brain imaging showed atrophy in all three affected individuals (**Table 2**). Homozygosity mapping identified multiple linkage regions with a maximum possible LOD score of 2.5, including a large region on chromosome 1. Whole exome sequencing identified a homozygous 2-base pair deletion in exon 1 of *EXOC8* in the linkage region (chr1:231471676-231471677 (hg19), CCT>C, Asp607Ter, **Figure 1D**), which is absent from normal controls (gnomAD database, Lek et al., 2016). This frameshifting deletion creates a premature stop codon at amino acid 607, short of the full-length protein (725 aa), and segregates perfectly with disease in this family. Two additional homozygous variants were detected in the family and determined not likely to be causative because one was present as a homozygous variant in gnomAD and the other was a missense variant not predicted to be pathogenic by several prediction tools.

In total, we report three novel, missense and splice site mutations in *EXOC7* and one novel truncating mutation in *EXOC8* in families with a recessive syndrome of brain atrophy, seizures, and developmental delay,

and in more severe cases microcephaly and infantile death (**Table 1**). The presence of cerebral atrophy in all families indicates neurodegeneration and suggests *EXOC7* and *EXOC8* are required for neuronal survival. Loss-of-function variants in *EXOC7* have not been previously linked to human disease, and we have recently reported one homozygous missense variant in *EXOC8* in a single case of Joubert syndrome (Dixon-Salazar et al., 2012).

***EXOC7* splice mutation reduces protein expression and eliminates one isoform**

We generated a minigene assay to model the exon 7 splice acceptor mutation from Family I and found this mutation disrupts splicing and decreases EXOC7 protein level. The minigene was constructed using 5 kb of genomic DNA from the human *EXOC7* locus spanning exon 6 to exon 9 (**Figure 2A**). RT-PCR of mRNA transcribed from the minigene plasmid expressed in mouse N2A cells revealed three splicing disruptions caused by the human mutation (**Figure 2A**). First, cDNA encoding the full-length transcript (including exons 6, 7, and 9) was isolated from wild-type minigene but completely absent from the mutant (**Figure 2A**). A low-abundance larger product that could not be sub-cloned for sequencing was found in wild-type and likely encodes a transcript including exons 6, 7, 8, and 9 (*, **Figure 2A**). Second, two novel out-of-frame splice forms that are predicted to encode early truncation mutations were found exclusively in mutant minigene cDNA (**Figure 2A**). Form A splices-in the last 37 bases of intron 6 causing a

frameshift which is predicted to create a premature stop codon at amino acid 286, well short of the full-length protein of 653 amino acids. Form B splices-out the first 14 bases of exon 7 causing a frameshift, predicted to create a premature stop codon at amino acid 290. An isoform that skips exon 7 and includes exons 6 and 9 was observed in both wild-type and mutant minigenes. These results suggest that this mutation eliminates expression of full-length EXOC7 protein and may reduce total amount of protein. Indeed, immunoblot of EXOC7 protein in HAP1 cells containing this mutation revealed a substantial decrease in amount full-length protein (**Figure 2B**). A HAP1 line was generated with CRISPR/Cas9 mutagenesis to encode the human mutation as a hemizygous variant. The full-length protein (including exon 7) was reduced by 50% in the mutant cell line compared to wild type (two-tailed t-test, p = 0.045) whereas expression of the isoform that skipped exon 7 was not changed (two-tailed t-test, p = 0.088, **Figure 2C**).

***EXOC7* is highly expressed in developing cerebral cortex**

EXOC7 is highly expressed in the developing human cortex, consistent with the affected individuals' phenotypes. *In situ* hybridization using RNAscope in human fetal cortex showed abundant *EXOC7* expression in the ventricular zone (adjacent to the ventricle and co-expressing *VIM*), the outer subventricular zone (co-expressing *TBR2*) and in the cortical plate (adjacent to the pial surface) (**Figures 3A, 3B**). RNA sequencing of human fetal cortex (Fietz et al., 2012) confirms this expression pattern with expression in the

ventricular zone and the inner and outer subventricular zones at a similar level as *ASPM*, a canonical microcephaly gene, and in the cortical plate (**Figure 3C**). *EXOC7* expression in both progenitors and postmitotic neurons suggests it has important roles in both cell types during cortical development. Notably, exon 7 of *EXOC7*, which contains a splice acceptor mutation in Family I, is differentially spliced in cortical progenitors compared to postmitotic cortical neurons. Using a previously published method (Zhang et al., 2016), we identified differentially spliced exons in the developing cortex with RNA sequencing of separated cortical progenitors and postmitotic neurons isolated from both developing mouse and human brain tissue. During fetal human cortical development (GW15), exon 7 is included in 93% of transcripts from the cortical plate and 47% of transcripts from ventricular zone (**Figure 3D**). Similarly, during cortical development in mice (E14.5), exon 7 is included in 87% of transcripts isolated from the cortical plate and 35% of transcripts from the ventricular zone (**Figure 3D**). The role of this differential splicing in the regulation of *EXOC7* function in development is unknown, but our evidence that the splicing mutation identified in Family I alters this differential expression by eliminating expression of the exon 7 included isoform (**Figure 2**) suggests it is pathogenic by disrupting cortical development.

***Exoc7* is essential for vertebrate embryonic development**

EXOC7 protein is highly conserved among vertebrates (**Figure 4A**). To further characterize the function of *EXOC7* in brain development, we examined *Exoc7* loss in both zebrafish and mouse. Mice deficient for *Exoc7* have been created by Taconic Biosciences and are reported to be homozygous lethal (personal communication). This is consistent with the phenotype for loss-of-function mutations in other exocyst components also reported to be early embryonic lethal (Mizuno et al., 2015; Friedrich et al., 1997), and suggests that the three human alleles identified retain some function and are partial loss-of-function.

To facilitate analysis of Exoc7 function during development, we took advantage of the ease of genome editing in the zebrafish. We created an *exoc7* mutant zebrafish with predicted loss-of-function of the encoded protein that allowed us to examine the function of *exoc7* in development. We used CRISPR/Cas9 mutagenesis to create a 1-bp deletion in exon 5 of *exoc7* that generates a predicted frameshift and subsequent nonsense mutation. This mutation is predicted to lead to a prematurely truncated protein at amino acid 185, well short of the full-length peptide at 735 (**Figure 4B**).

We found that *exoc7* is essential for zebrafish development. At 5 days post fertilization (dpf), approximately 25% of progeny from a heterozygous incross showed head edema and small eyes, consistent with Mendelian inheritance (**Figures 4C, D, G**). Genotyping confirmed that these phenotypes were associated with loss of *exoc7* and demonstrated that the

phenotype was highly penetrant (**Figure S3A**). These mutant fish die shortly after day 5, showing *exoc7* is essential for early zebrafish survival.

Quantification of the small eye phenotype revealed that the eye area was reduced by 26% in mutant fish (two-tailed t-test, 3.6×10^{-24}, **Figure S3B**). Broader characterization of the phenotype in *exoc7* mutant fish revealed general defects in head size although this was partially masked with the present edema. To account for the changes caused by the edema, we measured the distance from the outside of one eye to the other and then subtracted the regions of edema (**Figure 4C**). Even with this conservative measure, head diameter was 4% smaller in *exoc7* null fish compared to clutch controls (two-tailed t-test, $p = 6.8 \times 10^{-5}$, **Figure 4E**). We detected no difference in body length in mutant fish, suggesting that these defects are specifically caused by the loss of *exoc7* and not simply by developmental delay or allometric changes (two-tailed t-test, $p = 0.21$, **Figure 4F**).

Cellular defects in *exoc7* null developing telencephalon

To identify cellular mechanisms underlying microphthalmia and microcephaly in *exoc7* mutant zebrafish (**Figure 4G**), we measured apoptosis and progenitor cell count in the developing telencephalon. At 5 dpf, we found a 3-fold increase in the number of apoptotic cells (TUNEL stain) in the telencephalon of *exoc7* null zebrafish (Control n=5, *exoc7* KO n=5, two-tailed t-test, $p = 0.0023$, **Figure 4H**). At the same age, we also found a 53% decrease in the number of Sox2-positive telencephalon progenitor cells

(Control n=4, *exoc7* KO n=5, two-tailed t-test, p = 0.0019, **Figure 4I**). The number of Sox2-positive neuroprogenitors was also decreased in the retina of *exoc7* null fish, with a 76% decrease compared to controls (Control n=11, *exoc7* KO n=10, two-tailed t-test, $p = 3.0 \times 10^{-6}$, **Figures S3C**). Together, these results highlight specific cellular defects that drive microcephaly in zebrafish in the absence of *exoc7*, and further suggest that the atrophy and microcephaly observed in humans with *EXOC7* mutations reflect loss of proliferating progenitor cells and postmitotic neurons.

DISCUSSION

We identified three independent presumably hypomorphic mutations in *EXOC7* and one predicted null mutation in *EXOC8* causing a recessive human brain development disorder characterized by brain atrophy, seizures, and developmental delay and in more severe cases, microcephaly and infantile death. We show that *EXOC7*, a member of the mammalian exocyst complex, is highly expressed in developing human cortex. In addition, a zebrafish model of *Exoc7* deficiency recapitulates the human disorder with increased apoptosis and decreased progenitor cells during telencephalon development, suggesting that the brain atrophy in human cases reflects neuronal degeneration. These findings provide key inroads into understanding the role of the exocyst complex in the normal development of the cortex and complex neurodegenerative disorders in children.

Exocyst mutations cause a range of brain development disorders

Our work represents the first systematic genetic analysis of the role of exocyst components in human genetic disease. The three distinct alleles that we describe in *EXOC7* show a range of severity consistent with the degree to which they are likely to damage the protein, with the splicing mutation being most severe, a one amino acid deletion being less severe, and an amino acid substitution mutation being the mildest. However, all families share CNS disease and more specifically share cortical atrophy as a feature.

We also report a null mutation in *EXOC8* that is associated with severe phenotypes within this spectrum. Interestingly, we previously reported that a single affected individual with Joubert syndrome had a homozygous missense mutation (E265G) in *EXOC8* (Dixon-Salazar et al., 2012). This variant occurred at a highly conserved amino acid and was predicted to be damaging to protein function. Careful clinical review of the affected individuals we report herein confirms that they do not have the classic signs of Joubert syndrome. It is possible that these two alleles, E265G and Asp607Ter, lead to different clinical syndromes based on differing mutation severity, where a hypomorphic missense mutation causes Joubert syndrome and a null mutation causes cortical atrophy and microcephaly. Here we report that loss-of-functions mutations in either *EXOC7* or *EXOC8* lead to highly overlapping clinical features, suggesting perhaps that disruption of the exocyst complex broadly impairs normal cortical development. This is supported by previous work reporting an individual with Meckel-Gruber

Syndrome and microcephaly had a homozygous missense mutation (Gln578Arg) in another exocyst component, *EXOC4* (Shaheen et al., 2013). The exact mechanism for exocyst dysfunction causing microcephaly and cortical atrophy is not yet known, but previous work and our current results suggest the exocyst may be essential for multiple different molecular processes during cortical development. Joubert syndrome and Meckel-Gruber syndrome both have features of ciliopathies, disorders of cilia formation and function, and a zebrafish knockout of *exoc5* is also reported to cause a ciliopathy syndrome characterized by cardiac edema, small eyes with absent photoreceptor cells, and upward tail curvature (Lobo et al., 2017). Further, the exocyst has been reported to localize to the primary cilium and *EXOC5* is required for formation of a full-length cilium (Zuo et al., 2009). We find that loss of *EXOC7*, however, is not associated with features of ciliopathies in individuals with defective *EXOC7* or in zebrafish *exoc7* mutants. Thus, we propose that deficiencies in *EXOC7* lead to disrupted brain development characterized by atrophy and cell loss that may be a result of impaired RGC polarity and failed neuron migration that is distinct from ciliopathies caused by mutations in other exocyst members. Although other exocyst components have unique functions that have been previously described (Tanaka, 2017), the unique function of this gene remains unknown. We cannot rule out the possibility that cytokinesis, another reported function of the exocyst complex, is disrupted in the absence of *EXOC7* or *EXOC8*.

Exocyst complex in cortical development

Our results agree with previous studies of Exoc7 function in neurons and add new details for its role in brain development. Previous work reported that *in utero* electroporation of a different dominant negative *Exoc7* construct in developing mouse cortex impaired neuron migration (Letinic et al., 2009). *In vitro* knockdown of *Exoc7* in cultured hippocampal neurons disrupted polarization and prevented process outgrowth (Dupraz et al., 2009; Fujita et al., 2013). Additionally, the exocyst complex interacts with actin binding proteins required for cell polarity and migration and one such protein, Arp2/3, is required for cortical development. A conditional mouse knockout of *Arp2*/3 in neuroprogenitors showed severe cortical disorganization characterized by radial glia with truncated pial and basal processes, impaired migration of intermediate progenitors and postmitotic neurons, and abundant apoptosis (Wang et al., 2016). Here we find *exoc7* deficiency in the zebrafish developing telencephalon is also associated with abundant apoptosis.

We report the first identification of human mutations in an exocyst member, *EXOC7*, and show these mutations as well as a null mutation in another exocyst member, *EXOC8*, cause a neurodevelopmental syndrome of brain atrophy, seizures, and development delay with microcephaly and infantile death. This study exposes key, shared properties of two exocyst components in brain development. An *exoc7* loss-of-function zebrafish model we generated provides a new tool that can shed light on the mechanisms of

the exocyst complex in the developing brain supporting the role of *EXOC7* as the cause of this complex neurological disorder.

ACKNOWLEDGMENTS

The authors thank the families for their invaluable participation in our study. MEC was supported by F30 MH102909, Howard Hughes Medical Institute Medical Student Fellowship, and Nancy Lurie Marks Family Foundation Medical Student Fellowship. CAW was supported by R01 NS35129 and R01NS032457 from the NINDS, U01MH106883 from the NIMH, and the Allen Discovery Center program through The Paul G. Allen Frontiers Group. CAW and JG are Investigators of the Howard Hughes Medical Institute. KH and MPH were supported in part through funding from Children's Hospital Orthopaedic Surgery Foundation. This work was also supported by the Broad Center for Mendelian Genomics (UM1 HG008900), funded by the National Human Genome Research Institute with supplemental funding provided by the National Heart, Lung, and Blood Institute under the Trans-Omics for Precision Medicine (TOPMed) program and the National Eye Institute. EMD was supported by the National Institute of Biomedical Imaging and Bioengineering (NIBIB), of the National Institutes of Health under award number 5T32EB1680. The content is solely the responsibility of the authors and does not necessarily represent the official views of the National Institutes of Health.

AUTHOR CONTRIBUTIONS

MEC planned the work, conducted experiments, and wrote the manuscript. CAW directed the study and wrote the manuscript. XZ performed alternative splicing analysis. KH analyzed zebrafish experiments. RSS performed RNAscope. RSH, JNP, and GM performed linkage analysis and analyzed whole exome sequencing of families I and IV. DM and KJ performed linkage analysis and analyzed whole exome sequencing data of families II, III. SK and NH performed Sanger sequencing. MSZ, TS, LAG, MAS and AR performed clinical characterization and enrolled the families. AJB interpreted MRIs. LAG, GM, MPH, and JGG supervised and provided scientific input. All authors read and approved the manuscript.

DECLARATION OF INTERESTS

The authors have no interests to declare.

REFERENCES

Bhat, V., S. C. Girimaji, G. Mohan, et al. 2011. Mutations in WDR62, Encoding a Centrosomal and Nuclear Protein, in Indian Primary Microcephaly Families with Cortical Malformations. Clin. Genet. 80:532–540.

Bielas SL, Silhavy JL, Brancati F, et al. Mutations in INPP5E, encoding inositol polyphosphate-5-phosphatase E, link phosphatidyl inositol signaling to the ciliopathies. Nature genetics. 2009; 41(9):1032-6.

Bond, J., E. Roberts, G. H. Mochida, et al. 2002. ASPM Is a Major Determinant of Cerebral Cortical Size. Nat. Genet. 32:316–320.

Breuss, M., J. I.-T. Heng, K. Poirier, et al. 2012. Mutations in the ß-Tubulin Gene TUBB5 Cause Microcephaly with Structural Brain Abnormalities. Cell Rep. 2:1554–1562.

Bruce, A. and Rybak, A.P. CYB5D2 requires heme-binding to regulate HeLa cell growth and confer survival from chemotherapeutic agents. PLoS One. 2014 Jan 22;9(1):e86435.

Bultje RS, Castaneda-Castellanos DR, Jan LY, Jan YN, Kriegstein AR, Shi SH. Mammalian Par3 regulates progenitor cell asymmetric division via notch signaling in the developing neocortex. Neuron. 2009 Jul 30;63(2):189-202.

Chhetri RK, Amat F, Wan Y, Höckendorf B, Lemon WC, Keller PJ. 2015. Whole-animal functional and developmental imaging with isotropic spatial resolution. Nat Methods 12:1171-8.

Costa MR, Wen G, Lepier A, Schroeder T, Götz M. Par-complex proteins promote proliferative progenitor divisions in the developing mouse cerebral cortex. Development. 2008;135(1):11-22.

des Portes, V., J. M. Pinard, P. Billuart, et al. 1998. A Novel CNS Gene Required for Neuronal Migration and Involved in X-Linked Subcortical Laminar Heterotopia and Lissencephaly Syndrome. Cell 92:51–61.

Dickinson, M. E., Flenniken, A. M., Ji, X., Teboul, L., Wong, M. D., White, J. K., Meehan, T. F., Weninger, W. J., Westerberg, H., Adissu, H., Baker, C. N., Bower, L., and 73 others. High-throughput discovery of novel developmental phenotypes. Nature 537: 508-514, 2016.

Dillon GM, Tyler WA, Omuro KC, Kambouris J, Tyminski C, Henry S, Haydar TF, Beffert U, Ho A. CLASP2 Links Reelin to the Cytoskeleton during Neocortical Development. Neuron. 2017 Mar 22;93(6):1344-1358.e5.

Dixon-Salazar, T. J., Silhavy, J. L., Udpa, N., Schroth, J., Bielas, S., Schaffer, A. E., Olvera, J., Bafna, V., Zaki, M. S., Abdel-Salam, G. H., Mansour, L. A., Selim, L., and 17 others. Exome sequencing can improve diagnosis and alter patient management. Sci. Transl. Med. 4: 138ra78, 2012.

Essletzbichler P, Konopka T, Santoro F, et al. Megabase-scale deletion using CRISPR/Cas9 to generate a fully haploid human cell line. Genome research. 2014; 24(12):2059-65.

Fietz SA, Lachmann R, Brandl H, Kircher M, Samusik N, Schröder R, Lakshmanaperumal N, Henry I, Vogt J, Riehn A, Distler W, Nitsch R, Enard W, Pääbo S, Huttner WB. 2012. Transcriptomes of germinal zones of human and mouse fetal neocortex suggest a role of extracellular matrix in progenitor self-renewal. Proc Natl Acad Sci 109:11836-41.

Friedrich, G. A., Hildebrand, J. D., and Soriano, P. (1997). The secretory protein

Sec8 is required for paraxial mesoderm formation in the mouse. Dev. Biol. 192,
364–374.

Gleeson, J. G., K. M. Allen, J. W. Fox, et al. 1998. Doublecortin, a Brain-Specific Gene Mutated in Human X-Linked Lissencephaly and Double Cortex Syndrome, Encodes a Putative Signaling Protein. Cell 92:63–72.

Hu, W. F., O. Pomp, T. Ben-Omran, et al. 2014. Katanin P80 Regulates Human Cortical Development by Limiting Centriole and Cilia Number. Neuron 84:1240–1257.

Inoue, M., Chang, L., Hwang, J., Chiang, S.-H., Saltiel, A. R. The exocyst complex is required for targeting of Glut4 to the plasma membrane by insulin. Nature 422: 629-633, 2003.

Jayaraman, D., A. Kodani, D. M. Gonzalez, et al. 2016. Microcephaly Proteins Wdr62 and Aspm Define a Mother Centriole Complex Regulating Centriole Biogenesis, Apical Complex, and Cell Fate. Neuron 92:813–828.

Kim S, Lehtinen MK, Sessa A, et al. The apical complex couples cell fate and cell survival to cerebral cortical development. Neuron. 2010;66(1):69-84.

Lek M, Karczewski KJ, Minikel EV, et al. Analysis of protein-coding genetic variation in 60,706 humans. Nature. 2016; 536(7616):285-91.

Letinic K, Sebastian R, Toomre D, Rakic P. Exocyst is involved in polarized cell migration and cerebral cortical development. Proc Natl Acad Sci USA. 2009;106(27):11342-7.

Liu J, Zhao Y, Sun Y, et al. Exo70 stimulates the Arp2/3 complex for lamellipodia formation and directional cell migration. Curr Biol. 2012;22(16):1510-5.

Lizarraga, S. B., S. P. Margossian, M. H. Harris, et al. 2010. CDK5RAP2 Regulates Centrosome Function and Chromosome Segregation in Neuronal Progenitors. Development 137:1907–1917.

Lobo GP, Fulmer D, Guo L, et al. The exocyst is required for photoreceptor ciliogenesis and retinal development. J Biol Chem. 2017;292(36):14814-14826.

Mei K, Li Y, Wang S, et al. Cryo-EM structure of the exocyst complex. Nat Struct Mol Biol. 2018;25(2):139-146.

Mishra-Gorur, K., A. O. Çağlayan, A. E. Schaffer, et al. 2014. Mutations in KATNB1 Cause Complex Cerebral Malformations by Disrupting Asymmetrically Dividing Neural Progenitors. Neuron 84:1226–1239.

Miyata T, Kawaguchi A, Okano H, Ogawa M. 2001. Asymmetric inheritance of radial glial fibers by cortical neurons. Neuron 31: 727-41.

Mizuno, S., Takami, K., Daitoku, Y., Tanimoto, Y., Dinh, T. T., Mizuno-Iijima, S., et al. (2015). Peri-implantation lethality in mice carrying megabase-scale deletion on 5qc3.3 is caused by Exoc1 null mutation. Sci. Rep. 5:13632.

Muller J, Stoetzel C, Vincent MC, et al. Identification of 28 novel mutations in the Bardet-Biedl syndrome genes: the burden of private mutations in an extensively heterogeneous disease. Human genetics. 2010; 127(5):583-93.

Murthy, M., Garza, D., Scheller, R. H., Schwarz, T. L. Mutations in the exocyst component Sec5 disrupt neuronal membrane traffic, but neurotransmitter release persists. Neuron 37: 433-447, 2003.

Pagnamenta, A. T., J. E. Murray, G. Yoon, et al. 2012. A Novel Nonsense CDK5RAP2 Mutation in a Somali Child with Primary Microcephaly and Sensorineural Hearing Loss. Am. J. Med. Genet. A 158A:2577–2582.

Poirier, K., N. Lebrun, L. Broix, et al. 2013. Mutations in TUBG1, DYNC1H1, KIF5C and KIF2A Cause Malformations of Cortical Development and Microcephaly. Nat. Genet. 45:639–647.

Poirier, K., Y. Saillour, N. Bahi-Buisson, et al. 2010. Mutations in the Neuronal ß-Tubulin Subunit TUBB3 Result in Malformation of Cortical Development and Neuronal Migration Defects. Hum. Mol. Genet. 19:4462–4473.

Polgar N, Fogelgren B. Regulation of Cell Polarity by Exocyst-Mediated Trafficking. Cold Spring Harbor perspectives in biology. 2018; 10(3).

Reiner, O., R. Carrozzo, Y. Shen, et al. 1993. Isolation of a Miller–Dicker Lissencephaly Gene Containing G Protein ß-Subunit-Like Repeats. Nature 364:717–721.

Royer LA, Lemon WC, Chhetri RK, Wan Y, Coleman M, Myers EW, Keller PJ. 2016.
Adaptive light-sheet microscopy for long-term, high-resolution imaging in living organisms. Nat Biotechnol 34:1267-1278.

Scott EM, Halees A, Itan Y, et al. Characterization of Greater Middle Eastern genetic variation for enhanced disease gene discovery. Nature genetics. 2016; 48(9):1071-6.

Shaheen R, Faqeih E, Alshammari MJ, et al. Genomic analysis of Meckel-Gruber syndrome in Arabs reveals marked genetic heterogeneity and novel candidate genes. Eur J Hum Genet. 2013;21(7):762-8.

Thapa N, Anderson RA. 2012. PIP2 signaling, an integrator of cell polarity and vesicle trafficking in directionally migrating cells. Cell Adh Migr 6: 409–412.

Thapa N, Sun Y, Schramp M, Choi S, Ling K, Anderson RA. 2012. Phosphoinositide signaling regulates the exocyst complex and polarized integrin trafficking in directionally migrating cells. Dev Cell 22: 116–130.

Thauvin-Robinet C, Lee JS, Lopez E, et al. The oral-facial-digital syndrome gene C2CD3 encodes a positive regulator of centriole elongation. Nature genetics. 2014; 46(8):905-11.

Wang PS, Chou FS, Ramachandran S, et al. Crucial roles of the Arp2/3 complex during mammalian corticogenesis. Development. 2016;143(15):2741-52.

Wiegreffe C, Simon R, Peschkes K, Kling C, Strehle M, Cheng J, Srivatsa S, Liu P, Jenkins NA, Copeland NG, Tarabykin V, Britsch S. Bcl11a (Ctip1) Controls Migration of Cortical Projection Neurons through Regulation of Sema3c. Neuron. 2015 Jul 15;87(2):311-25.

Xiong X, Xu Q, Huang Y, Singh RD, Anderson R, Leof E, Hu J, Ling K. 2012. An association between type Ig PI4P 5- kinase and Exo70 directs E-cadherin clustering and epithelial polarization. Mol Biol Cell 23: 87 – 98.

Zhang X, Chen MH, Wu X, et al. Cell-Type-Specific Alternative Splicing Governs Cell Fate in the Developing Cerebral Cortex. Cell. 2016; 166(5):1147-1162.e15

Zuo X, Guo W, Lipschutz JH. The exocyst protein Sec10 is necessary for primary ciliogenesis and cystogenesis in vitro. Mol Biol Cell. 2009;20(10):2522-9.

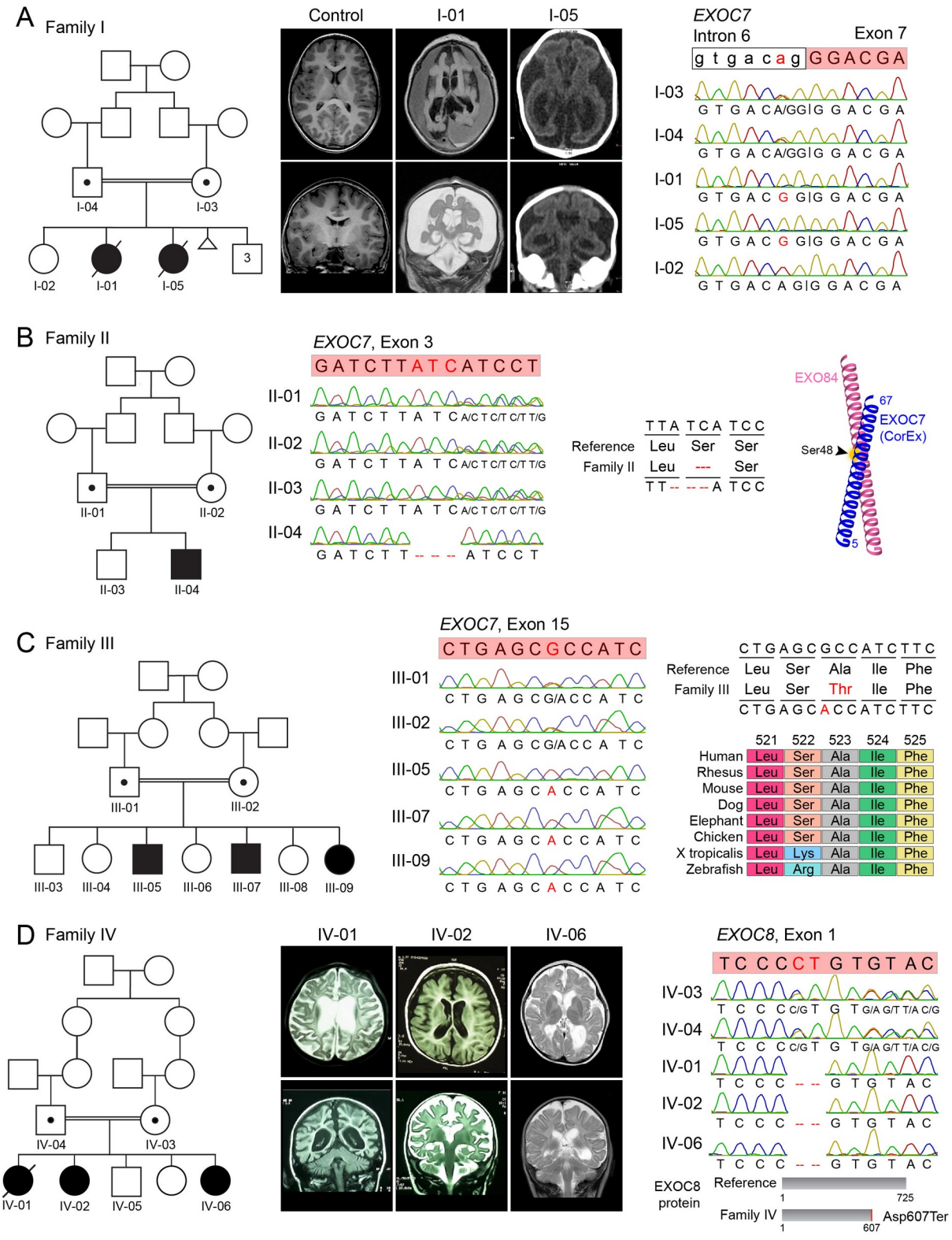
A
Family I
I-04
I-03
I-02
I-01
I-05
3
Control
I-01
I-05
EXOC7
Intron 6
Exon 7
g t g a c a g GGACGA
I-03
I-04
I-01
I-05
I-02
B
Family II
II-01
II-02
II-03
II-04
EXOC7, Exon 3
GATCTTATCATCCT
Reference
Family II
Leu
Ser
Ser
Leu

Ser
EXO84
67
EXOC7
(CorEx)
Ser48
5
C
Family III
III-01
III-02
III-03
III-04
III-05
III-06
III-07
III-08
III-09
EXOC7, Exon 15
CTGAGCGCCATC
Reference
Family III
Leu
Ser
Ala
Ile
Phe
Leu
Ser
Thr
Ile
Phe
CTGAGCACCATCTTC
521
522
523
524
525
Human
Rhesus
Mouse
Dog
Elephant
Chicken
X tropicalis
Zebrafish
D
Family IV
IV-04
IV-03
IV-01
IV-02
IV-05
IV-06
IV-01
IV-02
IV-06
EXOC8, Exon 1
TCCCCTGTGTAC
IV-03
IV-04
IV-01
IV-02
IV-06
EXOC8
protein
Reference
1
725
Family IV
1
607
Asp607Ter

Figure 1. *EXOC7* mutations cause a recessive brain development disorder

(A) Left, pedigree of Family I showing consanguineous parents and recessive inheritance of a lethal microcephaly in I-01 and I-05. Middle, coronal and axial brain MRI (I-01) or CT (I-05) show extremely simplified gyral pattern, small cortex, and fluid accumulation with age-matched normal MRI for comparison. Right, Sanger sequencing of *EXOC7* intron 6 / exon 7 boundary shows intronic A>G variant that mutates the canonical splice acceptor (ag|G to gg|G). This mutation is homozygous in affected individuals and segregates with disease. (B) Left, pedigree of Family II showing consanguineous parents and recessive inheritance of brain atrophy, microcephaly, and seizures in II-04. Middle, Sanger sequencing of *EXOC7* exon 3 reveals a homozygous 3-base pair ATC deletion in the affected individual that segregates with disease. Right, this deletion removes amino acid Serine 48, which is located in the CorEx domain of *EXOC7* and is responsible for binding to *EXO84* during exocyst assembly. (C) Left, pedigree of Family III showing consanguineous parents and recessive inheritance of brain atrophy and seizures in III-05, III-07, and III-09. Middle, Sanger sequencing of *EXOC7* exon 15 reveals a homozygous G>A variant in affected individuals that segregates with disease. Right, this variant changes amino acid 292, a highly conserved amino acid from humans to zebrafish, from alanine to threonine. (D) Family IV has recessive inheritance of a syndrome of developmental regression and delay, seizures, brain atrophy, and early death. Homozygosity mapping and

exome sequencing reveals a homozygous 2 base-pair deletion in *EXOC8* that causes early protein truncation.

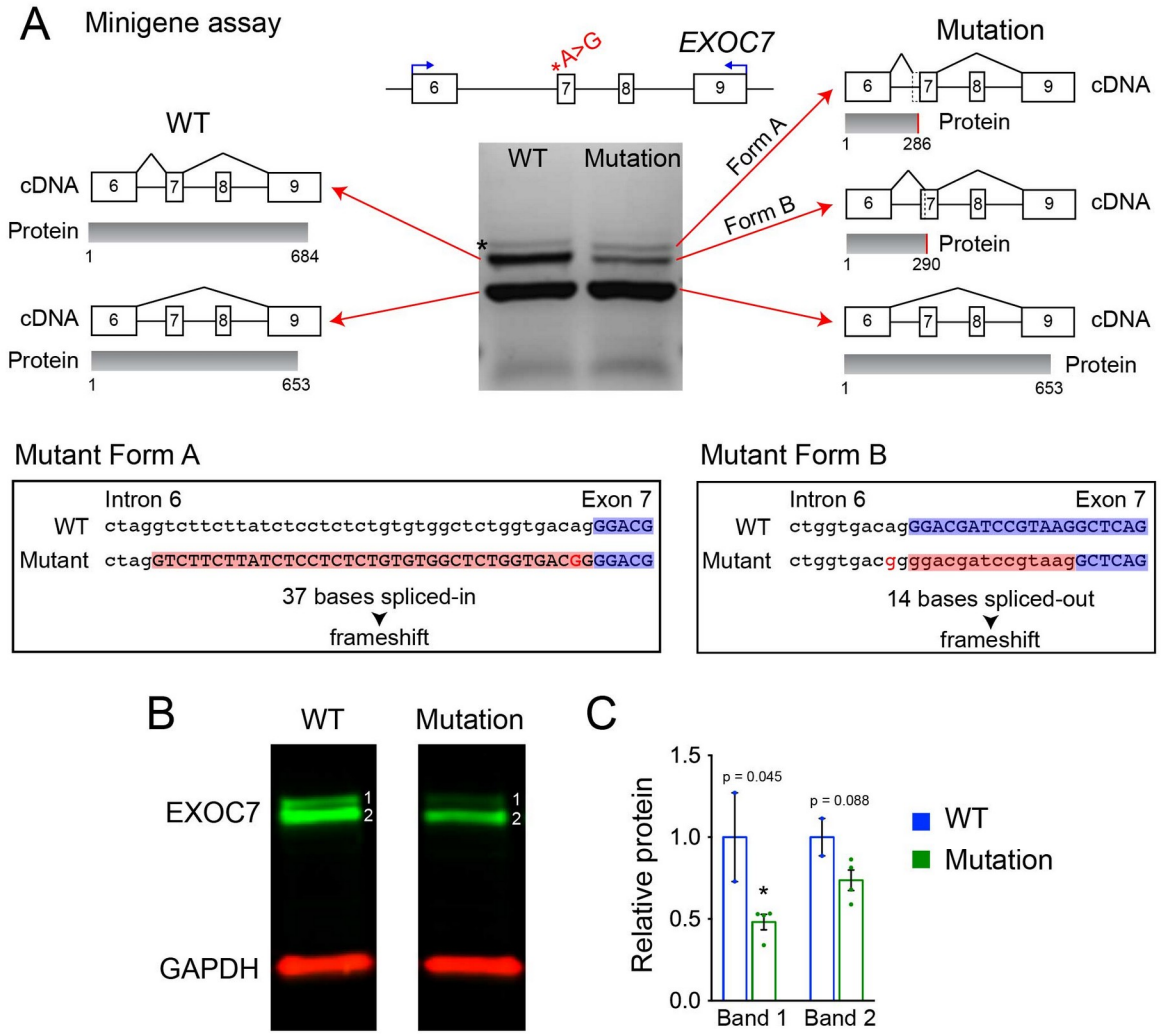

Figure 2. Family I exon 7 splice acceptor mutation disrupts splicing

(A) Top, diagram of *EXOC7* human minigene construct with splice acceptor mutation. Blue arrows mark RT-PCR primers used to generate cDNA products shown in gel image. Arrows from each band in gel point to splicing diagram determined by Sanger sequencing of the cDNA. WT minigene generated two in-frame isoforms (left), whereas mutant minigene generated one in-frame isoform and two novel out-of-frame isoforms (right). Two mutant isoforms encode novel stop codons that lead to premature protein truncation. *: low-

abundance product that could not be sub-cloned for sequencing and likely includes exons 6, 7, 8, and 9. (B) Immunoblot of EXOC7 protein in WT and mutant HAP1 cells showing difference in abundance of EXOC7 isoforms. GAPDH is a protein loading control. (C) Quantification of (B) showed significant 50% reduction of larger EXOC7 band (Band 1). P-values calculated by two-tailed t-test.

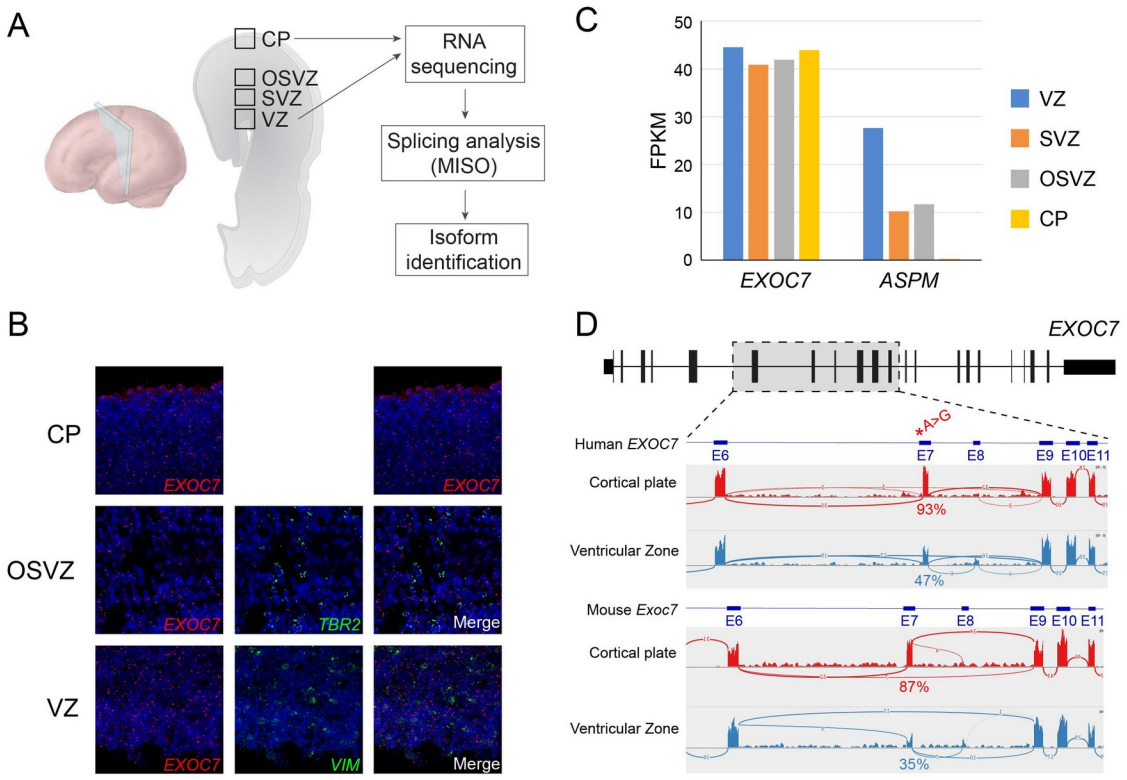

Figure 3. *EXOC7* is highly expressed in developing cortex

(A) Diagram of cortical section of human fetal cortex indicating locations of RNAscope imaging in (B) and RNA sequencing in (C). (B) RNAscope imaging of fetal human cortex shows EXOC7 expression in VZ and OSVZ, two progenitor zones and in CP, the location of post-mitotic neurons. (C) *EXOC7* is highly expressed in developing human cortex and shown in comparison to *ASPM*. Expression levels measured based on RNA-sequencing published in (Fietz et al., 2012). (D) RNA sequencing data from developing human fetal cortex (GW15) and mouse cortex (E14.5) showing differential inclusion of exon 7 in CP vs VZ.

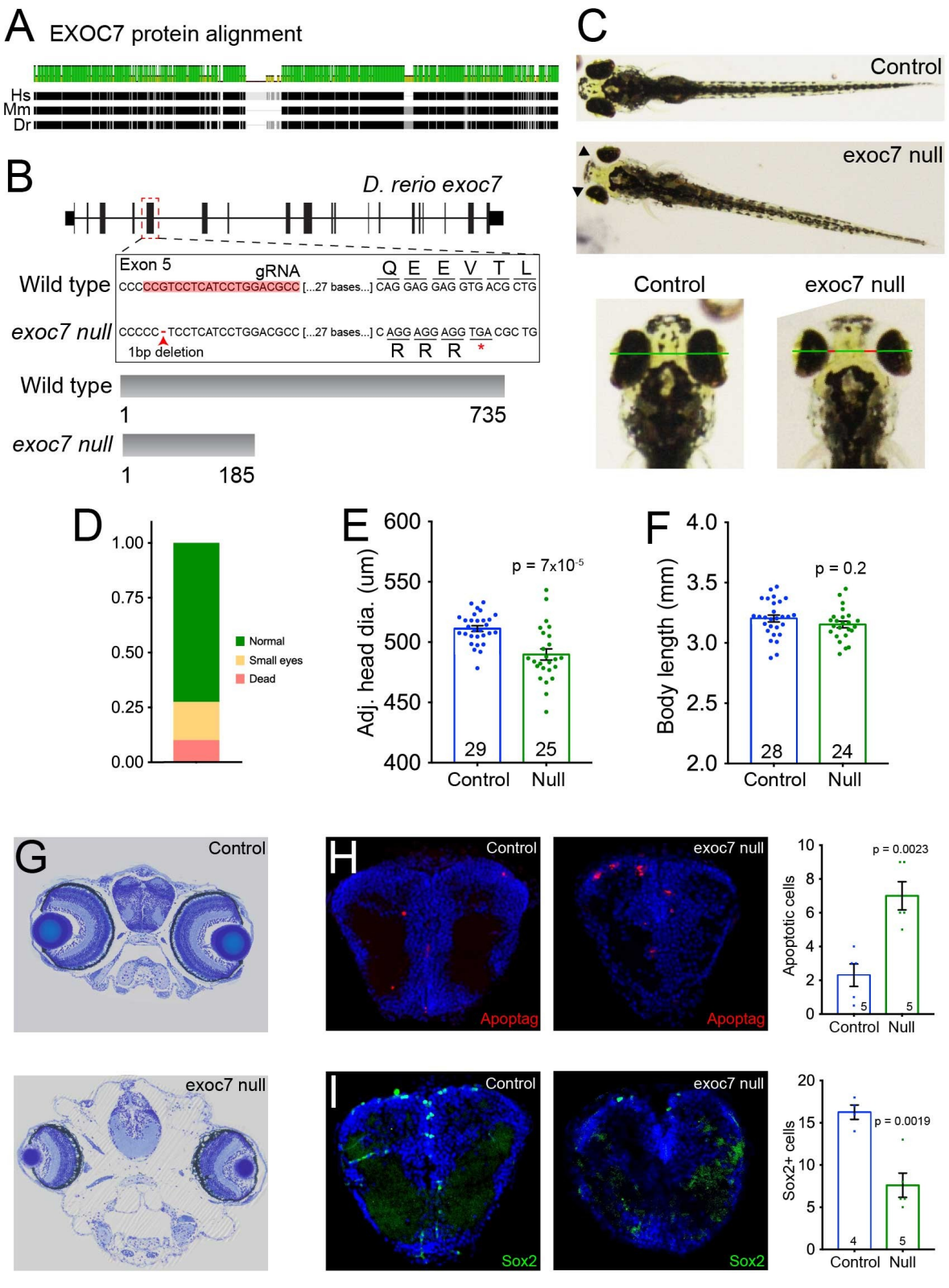
A
EXOC7 protein alignment
Hs
Mm
Dr
B
D. rerio exoc7
Exon 5
gRNA
Q E E V T L
Wild type
CCCCCGTCCTCATCCTGGACGCC [...27 bases...] CAG GAG GAG GTG ACG CTG
exoc7 null
CCCCC-TCCTCATCCTGGACGCC [...27 bases...] C AGG AGG AGG TGA CGC TG
1bp deletion
R R R *
Wild type
1
735
exoc7 null
1
185
C
Control
exoc7 null
Control
exoc7 null
D
1.00
0.75
0.50
0.25
0.00
Normal
Small eyes
Dead
E
Adj. head dia. (um)
600
550
500
450
400
p = 7x10-5
29
25
Control
Null
F
Body length (mm)
4.0
3.5
3.0
2.5
2.0
p = 0.2
28
24
Control
Null
G
Control
exoc7 null
H
Control
Apoptag
exoc7 null
Apoptag
Apoptotic cells
10
8
6
4
2
0
p = 0.0023
5
5
Control
Null
I
Control
Sox2
exoc7 null
Sox2
Sox2+ cells
20
15
10
5
0
p = 0.0019
4
5
Control
Null

Figure 4. *Exoc7* is essential for zebrafish telencephalon development

(A) Exoc7 amino acid sequence is highly conserved between human, mice, and zebrafish. (B) *exoc7* 1bp frameshift deletion mutation in exon 5 is confirmed by DNA sequencing and predicted to cause a frame shift and subsequently a protein truncation through a premature STOP codon at amino acid 186. (C) *exoc7* homozygous mutant fish have gross developmental abnormalities by 5 dpf notably small eyes and head edema. Diagram showing measurement of adjusted head diameter calculated by subtracting edema (red lines). (D) Heterozygous *exoc7* zebrafish crosses generated mutant fish (small eye/edema or dead) at expected Mendelian ratio. Genotyping confirmed that phenotypically mutant larvae were homozygous for the *exoc7* mutation. (E) Quantification of adjusted head diameter, which is significantly reduced in homozygous mutant fish. (F) Body length is not significantly changed in homozygous mutant fish. (G) Toluidine blue stain of 5 dpf wild-type and *exoc7* mutant zebrafish. (H) Apoptag staining shows a significant increase of apoptotic cells in the *exoc7* mutant telencephalon. (I) Immunohistochemical staining of neuronal progenitors using Sox2. The number of Sox2+ progenitors is significantly decreased in the *exoc7* mutant telencephalon. P-values calculated with two-tailed t-test.

Tables

	Family I	Family II	Family III	Family IV
Maximum LOD score	1.93	Singleton	2.9	2.5
Gene	*EXOC7*	*EXOC7*	*EXOC7*	*EXOC8*
Variant type	Splice mutation	In-frame deletion	Missense	Frameshift deletion
Variant	Exon 7 splice acceptor (C>T, c.809-2A>G)	Ser48del (GGAT>G)	Ala523Thr (C>T)	Asp607Ter (CCT>C)
Segregates in family	Yes	Yes	Yes	Yes
gnomAD frequency	2/251,414 alleles, heterozygous	2/276,426 alleles, heterozygous	2/277,066 alleles, heterozygous	Absent

Table 1. Variant summary for each family.

Individual	**I-01**	**I-05**
Gender	Female	Female
Gestational age at birth	Full term	33 weeks
Birth weight (z-score)	2 kg (-3.5)	1 kg (-2.4)
Birth length (z-score)	Not available	Not available
Birth head circumference (z-score)	31 cm (-2.7)	29 cm (-0.5)
Seizure onset, type	Birth, myoclonic seizures	Birth, myoclonic seizures
Developmental milestones	None	None
Muscle tone	Normal	Normal
Dysmorphisms	None	None
Brain imaging findings	Thin cortex, extremely simplified gyral pattern, moderately enlarged ventricles, diminished and watery white matter, very thin corpus callosum, thin optic nerves, absent basal ganglia and small thalami, large bilateral subdural hematomas, extremely thin cerebellar hemispheres and absent vermis, tiny brainstem with midline cleft (MRI)	Thin cortex, extremely simplified gyral pattern, moderately enlarged ventricles and markedly reduced white matter volume, profoundly small cerebellar hemispheres, vermis, midbrain, pons and medulla (CT)

Other findings	Arthrogryposis multiplex , normal CPK	Arthrogryposis multiplex
Life span	Died at 7 months of age	Died at 5 days of age

Individual	**II-02**
Gender	M
Age at most recent assessment	2y
Age at birth (e.g. term or 35 weeks)	Full term (mother took antibiotics at 4m gestation for abcess)
Birth weight	3kg (-0.9 SD)
Birth length	49.5cm (-0.5 SD)
Birth head circumference	34.2cm (-1 SD)
Seizure onset	6m, myoclonic and focal with versive head movement
Developmental features	Severe developmental delay
Muscle tone	Mild hypertonia
Dysmorphisms	No dysmorphic facies
Head circumference	45cm (-2.6SD)
Brain imaging findings	Central and cortical atrophy, especially temporal lobe

Individual	**III-05**	**III-07**	**III-09**
Gender	M	M	F
Age at most recent assessment	9y	6y	3y6m
Age at birth (e.g. term or 35 weeks)	37wks	35wks	35wks
Birth weight	2.7kg	2.4kg	2.2kg
Birth length	53cm	51cm	49cm
Birth head circumference	35cm	34cm	33cm
Seizure onset	6y	5y	3y
Developmental features	Mild delay	Mild delay	Moderate delay
Muscle tone	Normal	Normal	Normal
Dysmorphisms	No	No	Mild
Head circumference	50th centile	50th centile	40th centile

Brain imaging findings	Normal	Nonspecific atrophy	Atrophy

Individual	**IV-01**	**IV-02**	**IV-06**
Gender	Female	Female	Female
Gestational age at birth	Full term	Full term	Full term
Birth weight (z-score)	3.25 kg (-0.33)	3.25 kg (-0.33)	3 kg (-0.81)
Birth length (z-score)	48 cm (-0.65)	48 cm (-0.65)	47 cm (-1.1)
Birth head circumference (z-score)	33 cm (-1.2)	35 cm (0.11)	34 cm (-0.54)
Seizure onset, type	10m febrile onset, myoclonic and generalized tonic-clonic	13m, tonic spasms	In first year of life
Developmental milestones	Severe global developmental delay after loss of early acquired milestones, by 1y no longer able to sit, feed or communicate	Severe global developmental delay after loss of milestones (sat on own and stood with support at 9m), now bedridden, unable to feed and unresponsive to stimuli at 14y	Severe global developmental delay (no head control at 5m), able to bottle feed but placid with no interest in surroundings or grasping objects at 10m
Muscle tone	Hypertonia, muscle weakness	Muscle weakness	Hypotonia
Dysmorphisms	Round face, long eyelashes	Round face, long eyelashes	None noted
Head circumference	40 cm (-5.3SD) at 2y3m	39.5 cm (-12.9 SD) at 14y	39 cm (-4.7 SD) at 11m
Brain imaging findings	10m: Moderate brain atrophy, hypogenesis of corpus callosum, diffuse periventricular white matter signal intensity. 2y: Diffuse brain atrophy, abnormal white matter signal (most in parietal lobes)	9m: Generalized brain atrophy, hypogenesis of the corpus callosum	5m: Dilated lateral ventricles with choroid plexus cysts, prominent extra axial CSF spaces bilaterally, delayed myelination, thin corpus callosum

Other findings	Premature closure of cranial sutures, ptosis, vision loss, exotropia, optic disc pallor, optic nerve degeneration, excessive crying, severe spasticity, hyperreflexia and flexion contractures, hypsarrythmia, recurrent aspiration pneumonia, wasting (weight 12 kg, -5.5 SD at 14y)	Exotropia, excessive crying and extreme irritability, severe spasticity, hyperreflexia and flexion contractures, wasting (weight 13 kg, -5.3 SD at 14y)	Spasticity and hyperreflexia
Life span	Deceased at 14y	Alive at 14y	Alive at 11m

Table 2. Clinical features and imaging findings for all affected individuals.

Supplemental Materials

Note S1: Sanger sequencing of isoforms from minigene cDNA.

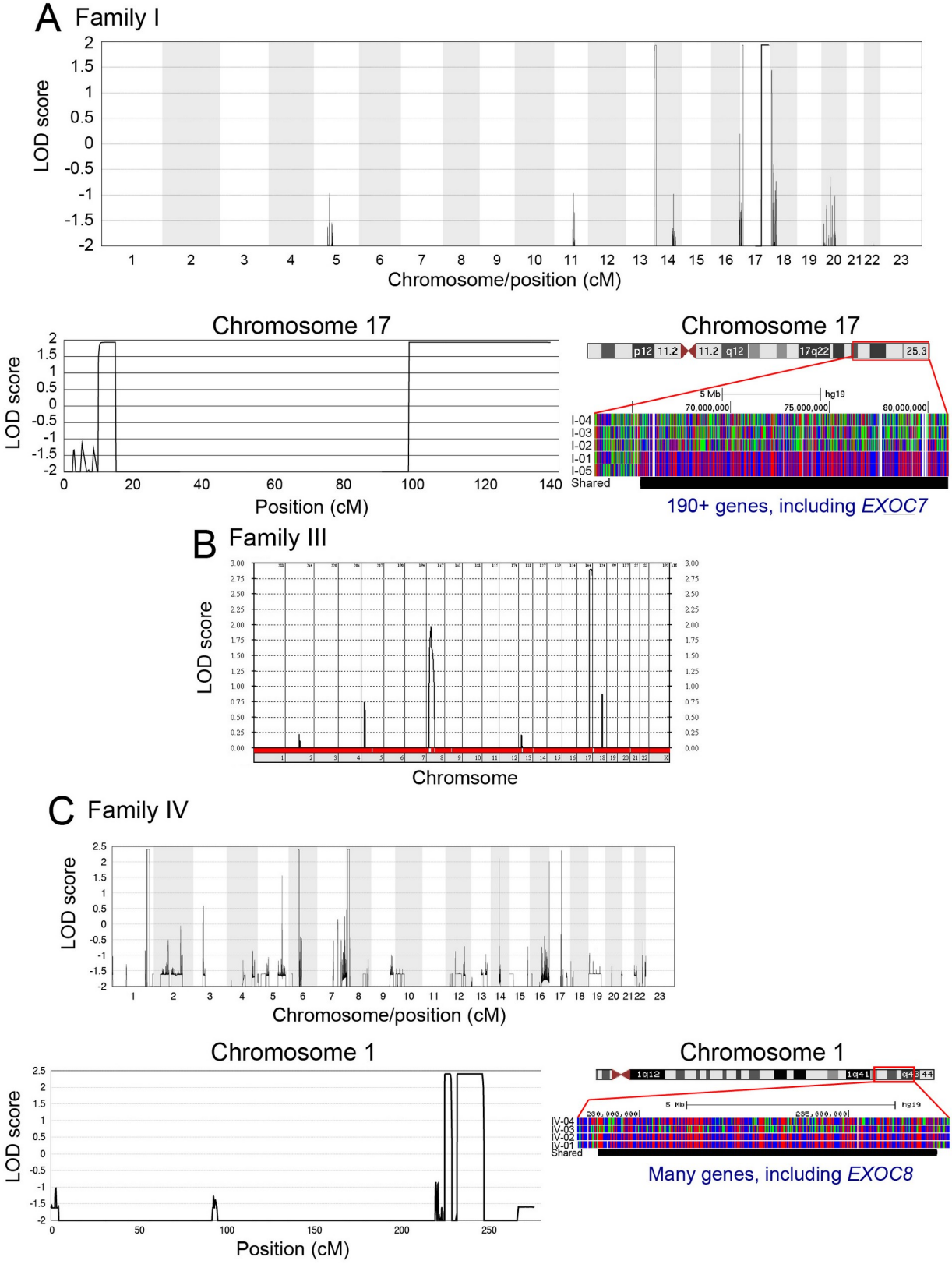

Figure S1. Linkage mapping of Families I, III, and IV.

(A) Family I showed linkage to a large region of homozygosity at the terminal q-arm of chromosome 17 with a maximum LOD score of 1.93. (B) Family III showed linkage to the terminal q-arm of chromosome 17 with a maximum LOD score of 2.9. (C) Family IV showed linkage to a large region of homozygosity on the q-arm of chromosome 1 with a maximum LOD score of 2.5.

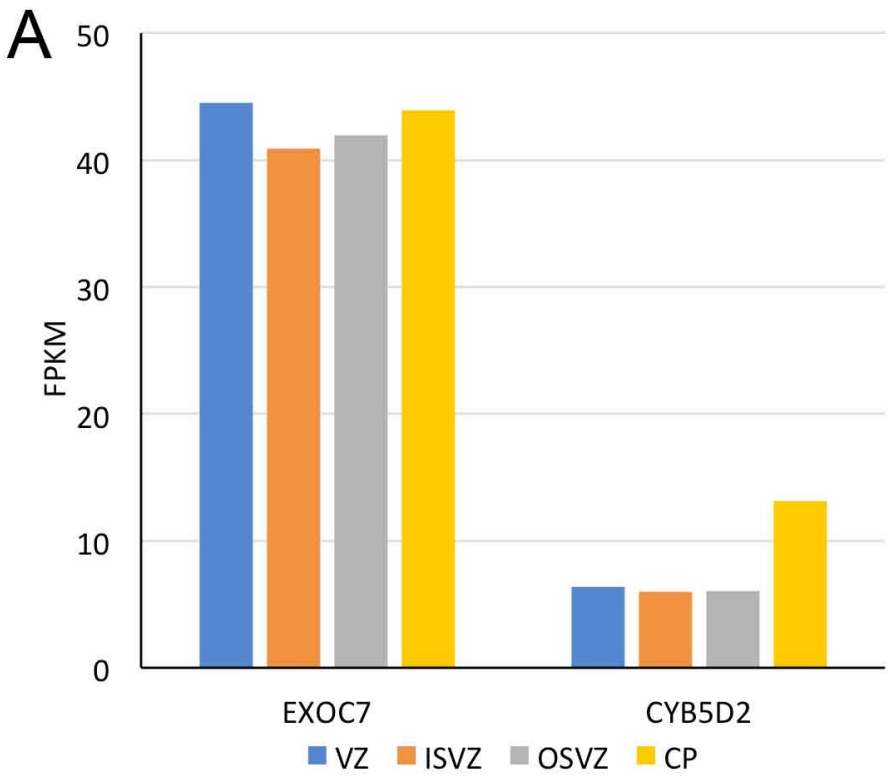

Figure S2. *CYB5D2* developing cortex expression is low

(A) *CYB5D2* expression in developing human cortex is dramatically lower than *EXOC7* expression (Fietz et al., 2012).

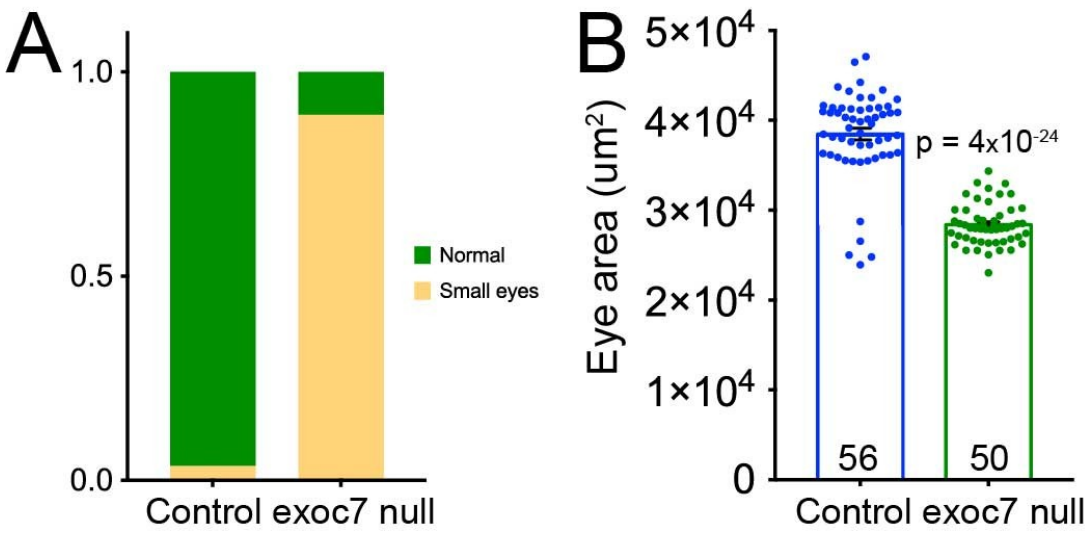

Figure S3. Eye size is decreased in exoc7 null zebrafish embryos